

International Conference on  
**CALIBRATION AND RELIABILITY  
IN GROUNDWATER  
MODELLING**



ModelCARE 90



The Hague, The Netherlands  
September 3-6, 1990

**VOLUME OF POSTER PAPERS**

Organised by

- National Institute of Public Health and Environmental Protection (RIVM), The Netherlands
- International Commission on Groundwater, of the International Association of Hydrological Sciences (IAHS)

**rivm**  
*research for  
man and environment*



INFLUENCE OF THE HYDRODYNAMIC COUPLING ON THE RESULTS  
OF AN OEDOMETRIC FINITE ELEMENT MODEL

A. DASSARGUES  
Laboratoires de Géologie de l'Ingénieur,  
d'Hydrogéologie et de Prospection Géophysique  
Université de Liège, BELGIUM.

ABSTRACT

Coupled and uncoupled finite element models have been tested to compute the subsidence of the central area of Shanghai (P.R.China), where a man-induced compaction is due to groundwater withdrawal.

The subsoil is composed of loose sediments with compressible layers of clay, muddy clay, loam, and with aquifer layers of silt and sand.

The oedometric law (elastoplasticity) has been adopted to simulate the geomechanical behaviour of the soils. Big differences are found in the results given by uncoupled and coupled models. In the studied case of Shanghai, the computed subsidence with the uncoupled model is reduced by nearly half when computed with coupled model.

The influences of the coupling on the results are detailed, analysed and explained mathematically and physically.

An example is taken from a tested column, located in the subsiding central area of Shanghai.

Conclusions are deduced from the discussion and a standard procedure of computation is inferred to calculate the subsidence of Shanghai with the maximum accuracy.

INTRODUCTION

The model exposed herein could be qualified of a "two-step" method according to Corapcioglu<sup>1</sup>. The aquifer flow equation is solved in a three-dimensional space and the assumed one-dimensional solid deformation is computed by one-dimensional consolidation equations.

The results of the 3D flow model are the time dependent boundary conditions of the 1D consolidation model. This consolidation model uses the oedometric elasto-plastic law coupled with vertical flow, including linear or non-linear analysis of the vertical permeability coefficient .

The developments presented hereafter have been implemented in the finite element code LAGAMINE which has been developed during the past seven years in the M.S.M. department, University of Liège<sup>2</sup>.

This model has been tested for computation of the land subsidence which has occurred severely (1.2 - 2.5 m) in Shanghai between 1920 and 1965. Since 1962-1963, the recharge during winters of the main aquifer has contributed to decrease the phenomena but a remanent consolidation of 2-3mm/year is still recorded.

## SYNTHESIS OF THE GEOLOGICAL, HYDROGEOLOGICAL AND GEOTECHNICAL DATA IN SHANGHAI

The 70 upper meters of the subsoil of Shanghai are composed of Quaternary deposits of the Yangtse River estuary. The center of the city has undergone a man-induced subsidence due to water pumping the confined multi-aquifer system located in these sediments.

A sedimentological study of the post-Pleistocene conditions of deposition and accumulation has been completed (Baeteman of the Belgian Geological Survey), using all the data prepared by the Shanghai Geological Center, including 5 new boreholes.

Accurate hydrogeological and geotechnical studies have been completed in order to determine hydrodynamic and geomechanic parameters in each formation.

To summarize, different units are distinguished (Dassargues et al.) from the top to the bottom (Fig. 1) :

- the superficial layer composed of slightly overconsolidated clay and loam, with sandy zones in some places forming the phreatic aquifer in direct relation with the Huang-Pu River.

- the first compressible layer (Holocene) composed of muddy clay deposits of estuarine tidal flats, this layer is highly compressible ( $0.4 \leq C_c \leq 1.2$ )

- the second compressible layer (Holocene) formed of supratidal silty clay deposits, with relatively high compressibility ( $0.3 \leq C_c \leq 1.2$ )

- the Dark Green Stiff Clay layer DGSC corresponding to deposits of fluvial clay flood basins. As indicated by the name, this layer is characterized by its high bearing capacity due to its previous compaction by dewatering, but in some places this overconsolidated layer is absent ( $0.2 \leq C_c \leq 0.4$ )

- the first aquifer composed of sand and silt with a low compressibility ( $0.2 \leq C_c \leq 0.3$ )

- the third compressible layer, clayey layer formed in subtidal and intertidal conditions, sensitive to compaction ( $0.3 \leq C_c \leq 1.2$ )

- the second aquifer, sandy layer deposited by estuarine conditions, may be considered as the main exploited aquifer. This layer possesses a high resistance and low compressibility ( $0.15 \leq C_c \leq 0.2$ )

It's to be noted that in some zones, the first and second aquifers may be connected and the third compressible may be at

Results of the oedometer and identification tests (Dassargués<sup>5</sup>) have shown that the first, second and third compressible layers are very slightly overconsolidated and DGSC layer strongly overconsolidated.

For the model, initial conditions of 1920 are chosen in perfect equilibrium, a triangular distribution of the initial effective stress ( $\sigma'_i$ ) is obtained assuming total saturation of the layers.

The preconsolidation effective stress is everywhere assumed equal to the initial effective stress except in the DGSC layer which is considered overconsolidated in 1920 with a mean ratio  $\frac{\sigma'_{prec}}{\sigma'_i} = 1.4$ .

For computation of the subsidence, the values of A (swelling constant) and C (compression constant) have been determined from  $C_s, C_c$  and the calculated initial void ratio of 1920 ( $e_i$ ).

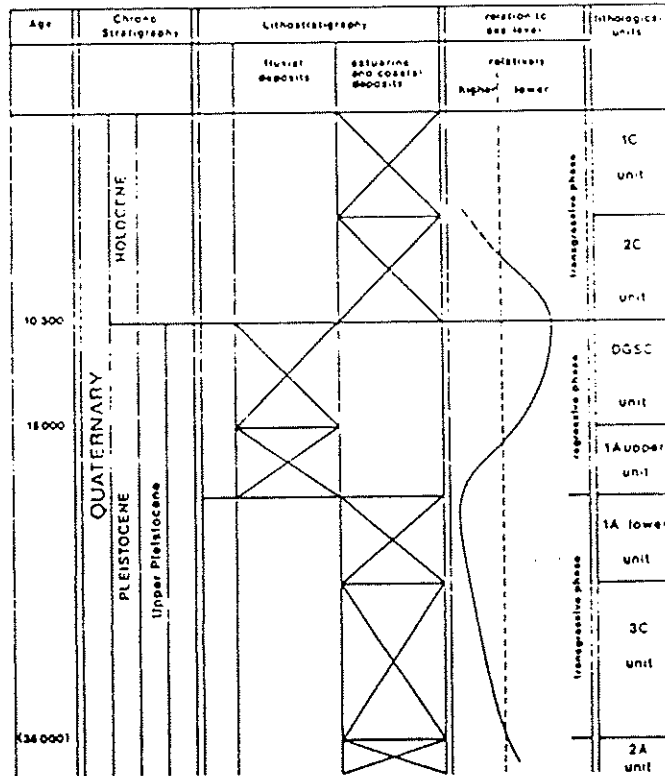


Figure 1 : Schematic lithological sequence of the upper 70 m in Shanghai (Baeteman<sup>3</sup>).

### VARIATION OF THE PERMEABILITY COEFFICIENT

Considering the variation of the permeability coefficient, the best tested empirical relation was the Nishida and Nakagawa equation. This equation links the permeability  $K$  to the void ratio  $e$  and plasticity index  $I_p$ .

This equation can be written:

$$K = \exp (\alpha_n \cdot e + \beta_n) \quad (\text{m/s}) \quad (1)$$

where  $\alpha_n = 2.3 / (C + D \cdot I_p)$

and  $\beta_n = (-27.6)$

$C$  and  $D$  are constants adapted to each layer

### VARIATION OF THE SPECIFIC STORAGE COEFFICIENT

The general expression of the specific storage is :

$$S_s = \rho \cdot g \cdot m_v = \rho \cdot g \cdot n \left( \beta - \beta_s + \frac{\alpha}{n} \right) \quad (2)$$

Usually  $\beta$  and  $\beta_s$  can be neglected in front of  $\alpha$  (Poland<sup>7</sup>), so that

$$S_s = \rho \cdot g \cdot \alpha \quad (3)$$

and  $\left\{ \begin{array}{l} S_s = \gamma_v / A \cdot \sigma' \quad (\text{in the elastic part}) \\ S_s = \gamma_v / C \cdot \sigma' \quad (\text{in the plastic part}) \end{array} \right. \quad (4)$

where  $A$  is the swelling constant  
 $C$  is the compression constant

In the coupled flow-compaction law, this variation is taken account assuming that the total quantity of water expelled during compaction ( $-f^v$ ) is equal to the time derivation of the strain

$$f^v = S_s \cdot \frac{\dot{p}}{\gamma_v} = - S_s \cdot \frac{\dot{\sigma}'}{\gamma_v} = - \dot{\epsilon} \quad (5)$$

### CHOICE OF THE COMPUTATIONAL SCHEMA

The permeability contrast between aquifers and aquitards is that the main flow can be considered as essentially influenced by horizontal transmissivities of the aquifers.

Consequently, the computational schema has been chosen as following :

- The flow model is a real 3D model (Dassargues<sup>8,9</sup>) with complete discretization of the different layers in the meshing network, values of  $K$  and  $S_s$  are chosen in the different units assuring a detailed spatial distribution. The pressure field in function of time and space is the result, but the values relative to the clay layers are not very significant because of the low permeability.
- The subsidence is computed coupling in the model, the vertical flow and the oedometric consolidation processes in the clayey layers.

- The pressures computed in the 3D model are introduced in the coupled model as variable prescribed pressures at the aquifer-aquitard boundaries.

Details about the formulation of the coupled element which is used, are given in the paper of Charlier et al<sup>10</sup>.

### CONSTITUTIVE LAW

For the geomechanical aspect, the oedometric law is written incrementally by the following formulation :

$$\dot{\epsilon} = \frac{1}{A} \frac{\dot{\sigma}'}{\sigma'} \quad \text{if } \sigma' < \sigma'_c \quad (6)$$

$$\begin{cases} \dot{\epsilon} = \frac{1}{C} \frac{\dot{\sigma}'}{\sigma'} \\ \dot{\sigma}'_c = \dot{\sigma}' \end{cases} \quad \text{if } \sigma' = \sigma'_c \quad (7)$$

For the hydrogeologic aspect, the equations are :

$$f^V = - \dot{\epsilon} \quad (5)$$

$$f = \frac{K}{\gamma_w} \text{grad } (p) + K \cdot \text{grad } (z) \quad (\text{Darcy's law}) \quad (8)$$

$$\text{and } K = \exp (\alpha_n \cdot e + \beta_n) \quad (1)$$

A relation between the void ratio variation and the strain variation can be easily established neglecting the compressibility of the grains.

$$\frac{\dot{e}}{(1 + e)} = \dot{\epsilon} \quad (9)$$

The constitutive laws allow to link  $\sigma$ ,  $\sigma'$ ,  $f$ ,  $f^V$ ,  $e$  and  $\sigma'_c$  to the main variables :  $\epsilon$  and  $p$ .

The parameters are  $A$  and  $C$  for the geomechanical aspect,  $\alpha$  and  $\beta$  for the hydrogeological aspect,  $\gamma_w$  and  $\gamma_s$  for the unit weight of water and dry solid.

As the problem is posed in transient conditions, the initial values of  $\sigma$ ,  $\sigma'$ ,  $p$ ,  $e$  and  $\sigma'_c$ , are needed.

### COMPARISON OF RESULTS

The Table 1 represents one of the columns which has been tested in the uncoupled case, the discretization of the column is taken from the 3D flow model (10 elements). For the coupled model, the discretization is more detailed (60 elements).

The geomechanical parameters are presented on Table 1 and the hydrogeological parameters on Table 2. In the compressible layers, the hydrogeological values, relative to the coupled model are more accurate than in the uncoupled model because equivalent values have to be chosen in the 3D flow model to represent globally these layers.

The coupling and non-linear analysis cause the variations of the specific storage ( $S_s$ ) and the permeability coefficient ( $K$ ); values of 1920 and 1960 are given on Table 2.

The water pressures are computed by the 3D flow model in the coupled conditions, and by the 1D flow-compaction model with variable prescribed pressures at the aquifer-aquitard limits (from the 3D flow model) in the coupled conditions. Fig. 2 shows the water pressure in the studied column, in 1960, for the uncoupled, the coupled and the coupled non-linear models.

Logically, it appears that the coupling creates less decrease of water pressure in the compressible layers. This is due mainly to the variations of the specific storage ( $S_s$ ) during the compaction process.

Absolute level	Geology	Geomechanical parameters		Discretizations		Coupled
				Uncoupled Flow	Uncoupled Compaction	
+5.0	clayey loam			1	6	
0.0	clay and silty sand	A = 45.9	C = 9.33			
-5.0						
-10.0	silty and sandy loam	A = 344.5	C = 5.75		2	
-15.0		A = 79.7	C = 13.3	1	2	
-20.0		A = 57.3	C = 9.5		2	
-25.0	clayey loam	A = 69.5	C = 11.5			2
-30.0		A = 28.9	C = 4.82	1	1	
-35.0		A = 27.1	C = 4.5		1	
-40.0		A = 26.4	C = 4.4		1	
-45.0	overconsolidated clay (O.G.S.C.)	A = 25.9	C = 4.7		1	6
-50.0						
-55.0	fine sand and silt (1 <sup>st</sup> and 2 <sup>nd</sup> aquifers are in connection)	A = 203	C = 24.6	6		36
-60.0						
-65.0						
-70.0						
-75.0						
-80.0						
-85.0						
-90.0						

Table 1 : Lithology and geomechanical parameters of the studied column.

Absolute level	Geology	S <sub>s</sub> m <sup>-1</sup>			K m/s		
		UNCOUPLED	COUPLED 1920	COUPLED 1960	UNCOUPLED	COUPLED NON-LINEAR 1920	COUPLED NON-LINEAR 1960
+5							
0	Clayey loam		1.53	0.32			
-5		4 10 <sup>-3</sup>			1 10 <sup>-8</sup>	1 10 <sup>-8</sup>	0.9 10 <sup>-8</sup>
-10	Clay and silty sand		9.7 10 <sup>-3</sup>	9.5 10 <sup>-3</sup>			
-15			1.57 10 <sup>-2</sup>	1.5 10 <sup>-2</sup>		2.5 10 <sup>-9</sup>	2.4 10 <sup>-9</sup>
-20	Silty and sandy loam	0.2 10 <sup>-3</sup>	1.15 10 <sup>-2</sup>	1.15 10 <sup>-2</sup>	5 10 <sup>-6</sup>	2.8 10 <sup>-10</sup>	2.7 10 <sup>-10</sup>
-25			5.2 10 <sup>-3</sup>	5.0 10 <sup>-3</sup>		1 10 <sup>-7</sup>	0.8 10 <sup>-7</sup>
-30			4.2 10 <sup>-3</sup>	4.0 10 <sup>-3</sup>			
-35			5.9 10 <sup>-3</sup>	5.2 10 <sup>-3</sup>			
-40	Clayey loam	4.1 10 <sup>-3</sup>	4.5 10 <sup>-3</sup>	4.3 10 <sup>-3</sup>		2.7 10 <sup>-9</sup>	2.3 10 <sup>-9</sup>
-45			3.4 10 <sup>-3</sup>	3.2 10 <sup>-3</sup>			
-50			8.0 10 <sup>-3</sup>	7.7 10 <sup>-3</sup>	5 10 <sup>-9</sup>	1.3 10 <sup>-9</sup>	1 10 <sup>-9</sup>
-55			2.2 10 <sup>-3</sup>	6.8 10 <sup>-3</sup>		4.1 10 <sup>-10</sup>	3 10 <sup>-10</sup>
-60			7.7 10 <sup>-3</sup>	7.3 10 <sup>-3</sup>		1.6 10 <sup>-9</sup>	1 10 <sup>-9</sup>
-65			7.0 10 <sup>-3</sup>	6.4 10 <sup>-3</sup>		2.3 10 <sup>-10</sup>	1.2 10 <sup>-10</sup>
-70			7.2 10 <sup>-3</sup>	6.5 10 <sup>-3</sup>			
-75			6.5 10 <sup>-3</sup>	5.75 10 <sup>-3</sup>			
-80			6.1 10 <sup>-3</sup>	5.4 10 <sup>-3</sup>			
-85			6.7 10 <sup>-3</sup>	7.2 10 <sup>-3</sup>			
-90			4.7 10 <sup>-3</sup>	4.4 10 <sup>-3</sup>			
	SSC	0.1 10 <sup>-3</sup>	10.5 10 <sup>-4</sup>	6.9 10 <sup>-4</sup>	1 10 <sup>-5</sup>	1.2 10 <sup>-5</sup>	1.0 10 <sup>-5</sup>
	Fine sand	0.2 10 <sup>-5</sup>			5 10 <sup>-4</sup>		
	and silt		6.7 10 <sup>-4</sup>	6.0 10 <sup>-4</sup>		7.5 10 <sup>-4</sup>	7.5 10 <sup>-4</sup>
		0.2 10 <sup>-5</sup>			1 10 <sup>-4</sup>		
			7.4 10 <sup>-4</sup>	5.5 10 <sup>-4</sup>			
		0.2 10 <sup>-5</sup>			7.5 10 <sup>-4</sup>		
			7.0 10 <sup>-4</sup>	5.3 10 <sup>-4</sup>			
		0.2 10 <sup>-5</sup>			7.5 10 <sup>-4</sup>		
			5.5 10 <sup>-5</sup>	4.2 10 <sup>-4</sup>			

Table 2 : Hydrodynamic parameters in the studied column.

These differences in the water pressure will constitute the main cause of the different computed subsidences.

The small divergences between linear and non-linear computations are due to the effects of the permeability variations.

The diagram of  $\dot{\epsilon}$  (variation of strain) in 1960 (Fig.3) clearly shows variable differences between results given by uncoupled, coupled and coupled non-linear models.

By equation (7) of the constitutive law and equation (4) of the specific storage definition, we obtain :

$$\dot{\epsilon} = S_s \frac{\sigma^i}{\gamma_w} \quad (10)$$



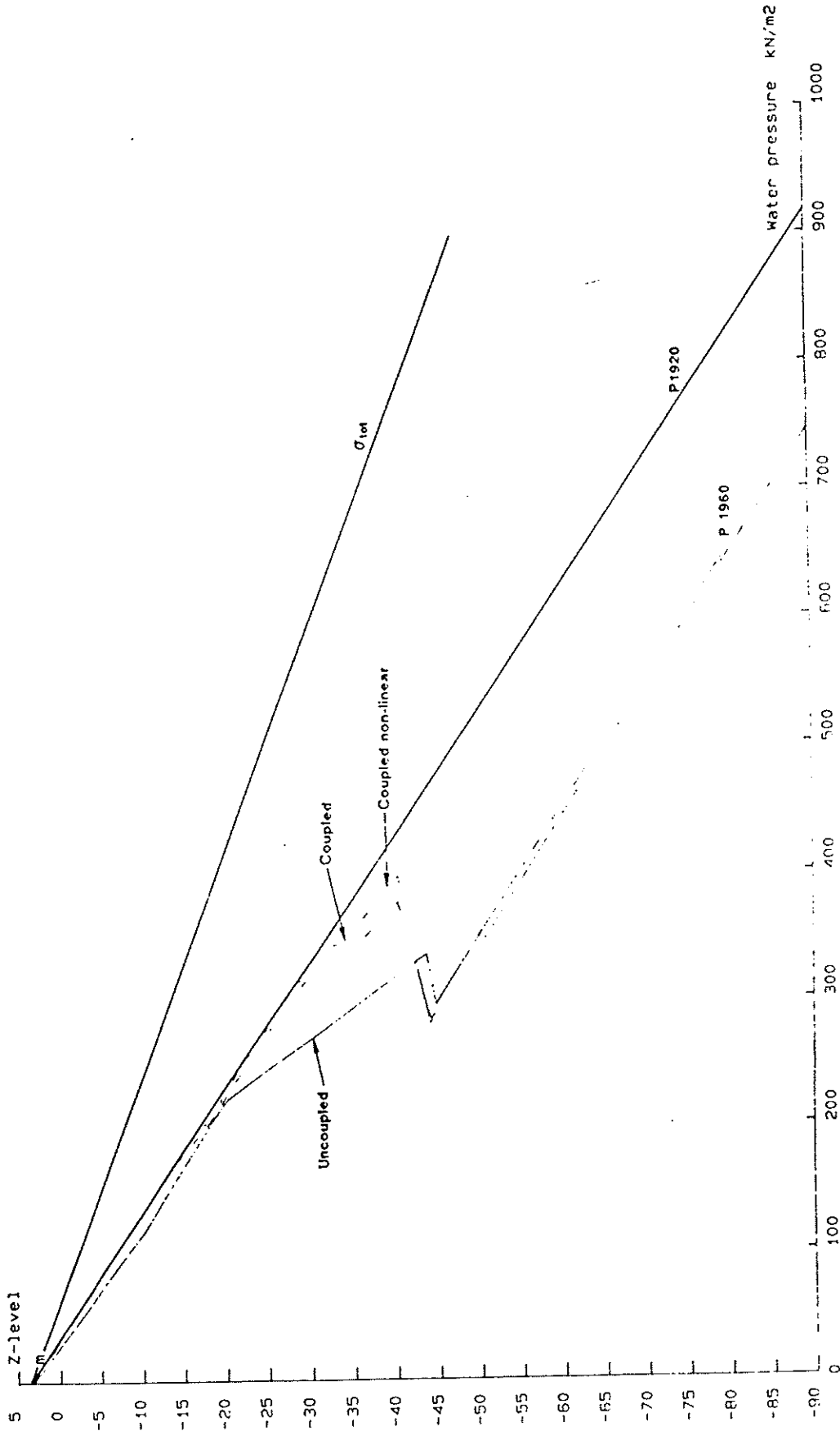


Figure 2 : Water pressure in function of depth at the studied column, in 1960.

In the uncoupled case,  $S_s$  and  $\gamma_w$  are considered constant and this expression can be written :

$$\int_{\varepsilon(t)}^{\varepsilon(t+\Delta t)} d\varepsilon = \frac{S_s}{\gamma_w} \int_{\sigma'(t)}^{\sigma'(t+\Delta t)} d\sigma' \quad (11)$$

By integration and considering only plasticity, we have :

$$\varepsilon(t + \Delta t) - \varepsilon(t) = \frac{1}{C \cdot \sigma'_s} \left( \sigma'(t + \Delta t) - \sigma'(t) \right) \quad (12)$$

where  $\sigma'_s$  is a constant chosen implicitly,

depending of the choice of the constant  $S_s$  value in each layer.

In the coupled case, only  $\gamma_w$  can be considered constant, replacing  $S_s$  by its value in (4) and assuming only plasticity :

$$\int_{\varepsilon(t)}^{\varepsilon(t+\Delta t)} d\varepsilon = \frac{1}{C} \int_{\sigma'(t)}^{\sigma'(t+\Delta t)} \frac{d\sigma'}{\sigma'} \quad (13)$$

By integration :

$$\varepsilon(t + \Delta t) - \varepsilon(t) = \frac{1}{C} \ln \left( \frac{\sigma'(t + \Delta t)}{\sigma'(t)} \right) \quad (14)$$

Comparing the equations (12) and (14), one can understand immediately why large differences may be constated in the  $\dot{\varepsilon}$  diagram :

- a. the  $\sigma'(t + \Delta t)$ ,  $\sigma'(t)$  values are not equal in the uncoupled and coupled cases
- b. the mathematical expression of  $\dot{\varepsilon}$  is quite different in (12) and (14) and the following terms are still to be compared:

$$\frac{1}{\sigma'_s} \left( \sigma'(t+\Delta t) - \sigma'(t) \right) \quad \text{and} \quad \ln \left( \frac{\sigma'(t+\Delta t)}{\sigma'(t)} \right)$$

As  $|a - b| > \left| \ln \frac{a}{b} \right| \quad \forall a, b > 1$ , we can conclude that excepting the preponderant influence of  $\sigma'_s$ , the uncoupled term will be normally greater then the coupled term.

- c. the constant  $\sigma'_s$  (of the uncoupled case) depends of the artificial choice of the constant  $S_s$  value in the layer

The non-linearity of  $K$  changes the water pressure distribution and then the effective stress distribution. This influence leads to reduce the decrease of pressure (the increase in effective stress), that's why the variation of strain and the strain are smaller than in the other cases (Fig.3).

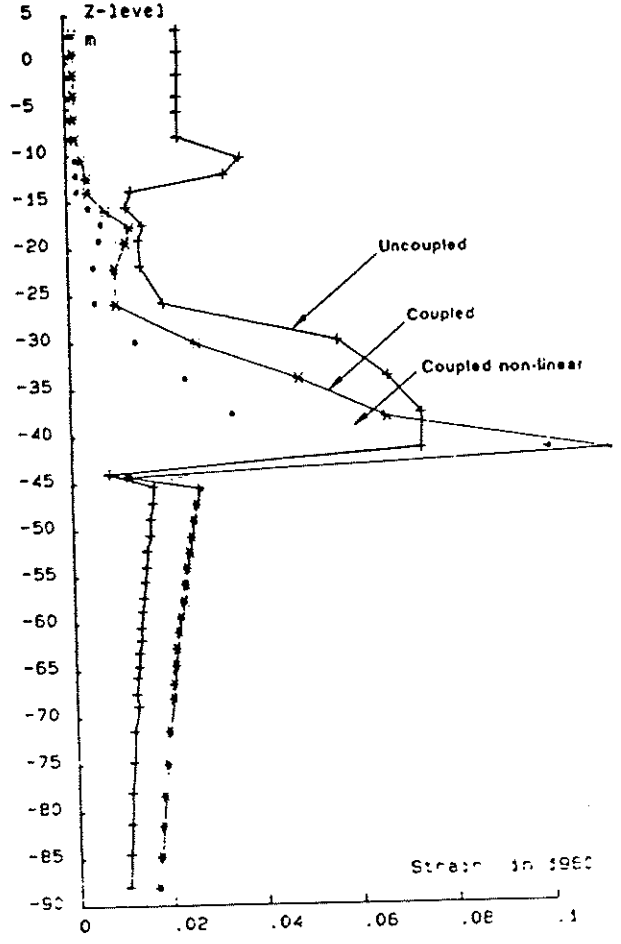
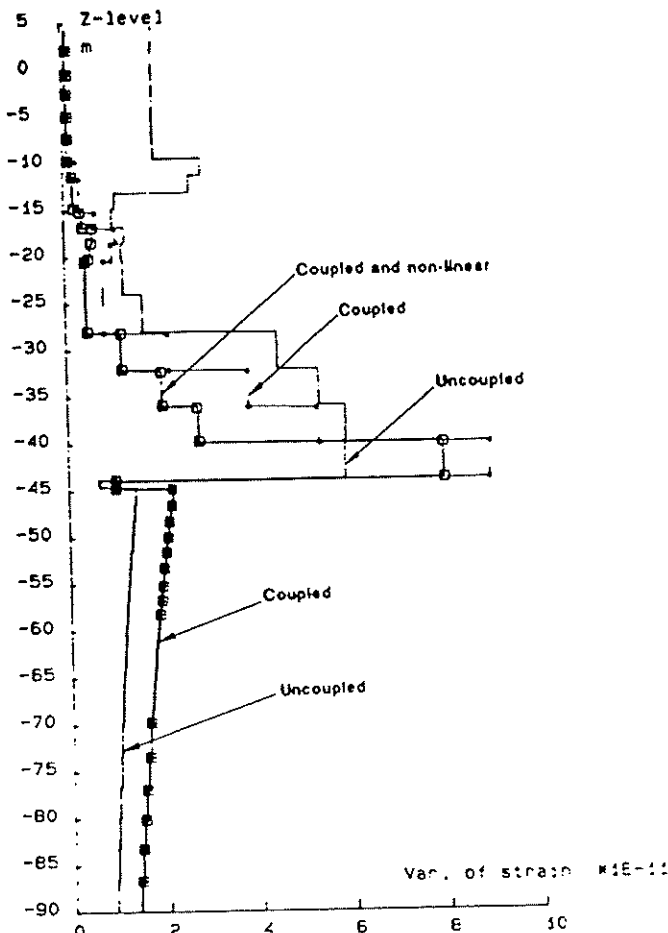


Figure 3 : The variation of strain in function of depth in 1960.

The strain in function of depth in 1960.

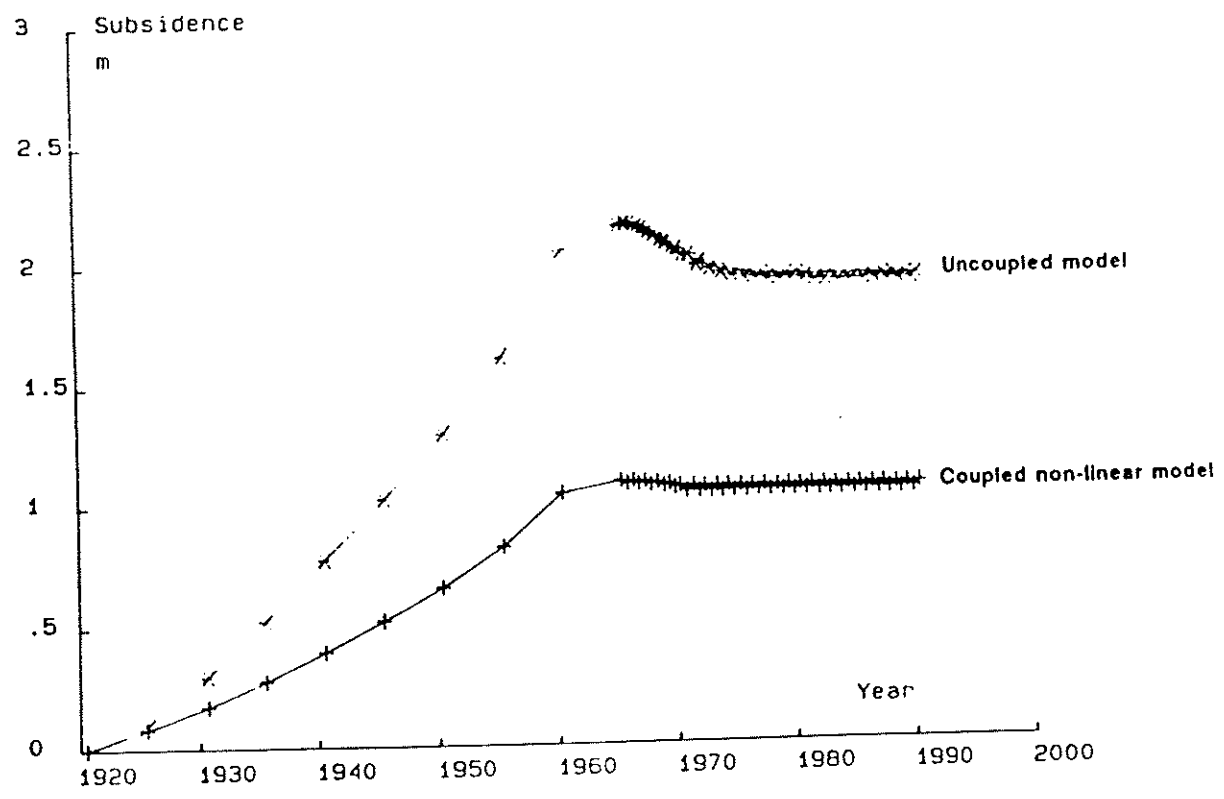


Figure 4 : Computed total subsidence in the studied column.

As a final result, Fig. 4 shows the difference in the computed subsidence (in function of time) in this column of the central area of Shanghai. A difference about 0.875 m is shown for the final values, corresponding to a relative error of about 83 % between uncoupled model and coupled non-linear model.

## CONCLUSIONS

The comparison of the uncoupled and coupled laws, with linear and non-linear analysis of the permeability coefficient, in this flow-compaction model has underlined different trends and results :

- The flow-compaction coupling introduces a non-linearity of the specific storage as  $S_s$  is linked to  $\sigma'$ . Theoretically, this coupling doesn't influence the spatial distribution of the decrease in water pressures if we consider quasi steady conditions (the specific storage affects only the transient term in the general diffusion equation). Nevertheless, in our case, the distributions of  $\epsilon$  and  $c$  (Fig.3) depend of the transient conditions imposed to the problem from 1920 to 1960, so that  $\sigma'_{\text{coupled}} \neq \sigma'_{\text{uncoupled}}$  even with linearity of K.
- The non-linearity of K induces additional changes in the water pressures especially in the compressible layers.
- The main difference in the computed subsidences is due to the introduction of an artificial specific storage coefficient, which is constant in the uncoupled conditions. If the same initial specific storage coefficients are chosen for both uncoupled and coupled models, the subsidence computed with uncoupled law is strongly smaller.

These conclusions are demonstrating that a detailed study is needed to choice the best procedure to be adopted in order to reduce, in each case, the approximations and to match a maximum to the reality of the involved processes.

Entire and detailed results of the study completed on the case of Shanghai are exposed and discussed in another paper<sup>11</sup>.

## ACKNOWLEDGEMENTS

This work has been carried out under an International Cooperative Agreement between the Ministry of Geology and Mineral Resources of People's Republic of China and the Services of Scientific Policy and Planning of the Prime Minister of Belgium.

The author is grateful to Dr. R.CHARLIER (University of Liège) who have provided the numerical code LAGAMINE and have developed it for the coupling and non-linear aspects.

Thanks must also be recorded to Professor A.MONJOIE (University of Liège) who have directed the research and to the Chinese engineers of the Shanghai Geological Center for their participation to the works and discussions during all the study.

## LIST OF KEYWORDS

Flow-compaction, modelling, coupled model, non-linearity, subsidence modelling, non-linear analysis, hydrodynamic parameters, groundwater, consolidation model.

## REFERENCES

1. CORAPCIOGLU M.Y., Land subsidence , A State-of-the-Art re-  
in Fundamentals of Transport Phenomena in Porous media, ed  
by Bear J. and Corapcioglu M.Y., NATO ASI Series, Series E  
Applied Sciences n°82 pp 369-444, 1984.
2. CHARLIER R., Approche unifiée de quelques problèmes non-li-  
res de mécanique des milieux continus par la méthode des é-  
ments finis (code LAGAMINE). Thèse de Doctorat, Collectio  
publication de la Faculté des Sciences Appliquées, n°109,  
Université de Liège, Belgique, 1987.
3. BAETEMAN C., BORREMANS E., LIN J. X., and HUANG H. Z.,  
Land Subsidence in Shanghai, The upper Quaternary deposits  
the Changjiang coastal plain (Shanghai area), edited by  
Monjoie A. ...in preparation 1990.
4. DASSARGUES A., SCHROEDER Ch. and MONJOIE A.  
The hydrogeology and engineering geology of the Shanghai a  
Laboratoires de Géologie de l'Ingénieur, d'Hydrogéologie e  
de Prospection géophysique, Rapport SPPS 891, unpublished,
5. DASSARGUES A., BIVER P., SCHROEDER Ch., and LI X.L.,  
Land Subsidence in Shanghai, Applying LAGAMINE Code to com  
land subsidence in Shanghai edited by Monjoie A.  
...in preparation 1990.
6. NISHIDA Y. and NAKAGAWA S., Water permeability and plastic  
index of soils, in Land Subsidence IAHS-UNESCO, Publ. n°89  
AIHS(2) : 573-578, 1969.
7. POLAND J.F., Mechanics of land subsidence due to fluid  
withdrawal, in Guidebook to studies of land subsidence due  
ground-water withdrawal, UNESCO, 1984.
8. DASSARGUES A., RADU J-P., and CHARLIER R.,  
Finite elements modelling of a large water table aquifer i  
transient conditions, Adv. in Water Resources, Vol. 11, n°  
1988.
9. DASSARGUES A., BOLLY P.Y. and MONJOIE A.,  
Finite difference and finite element modelling of an aquif  
Cretaceous chalk, Proceedings of Numerical Methods in  
Geomechanics, Innsbruck, Balkema, 1988.
10. CHARLIER R., RADU J-P and LI Q.F.,  
Land Subsidence in Shanghai, LAGAMINE Finite Element Code  
applied in land subsidence computations, edited by Monjoie  
...in preparation 1990.
11. DASSARGUES A., RADU J-P, CHARLIER R., LI Q.F. and LI X.L.,  
Land Subsidence in Shanghai, Computed subsidences - Discus  
of the results, edited by Monjoie A., ...in preparation